NeuroImage 45 (2009) 891–902

Contents lists available at ScienceDirect

NeuroImage

journal homepage: www.elsevier.com/locate/ynimg

[18F]Flumazenil binding to central benzodiazepine receptor studies by PET – Quantitative analysis and comparisons with [11C]flumazenil –

Ikuo Odano [a,c,*], Christer Halldin [a], Per Karlsson [a], Andrea Varrone [a], Anu J. Airaksinen [a,d], Raisa N. Krasikova [a,e], Lars Farde [a,b]

[a] Psychiatric Section, Department of Clinical Neuroscience Karolinska Institute, SE-17176, Stockholm, Sweden
[b] AstraZeneca R&D, SE-15185 Södertälje, Sweden
[c] Division of Functional Imaging, Department of Sensory and Integrative Medicine. Niigata University Graduate School of Medicine and Dental Sciences, Asahimachi-dori Niigata, 951-8510, Japan
[d] Laboratory of Radiochemistry, Department of Chemistry, University of Helsinki, Finland
[e] Institute of Human Brain, Russian Academy of Science, St. Petersburg, Russia

ARTICLE INFO

Article history:
Received 15 August 2008
Revised 25 November 2008
Accepted 1 December 2008
Available online 24 December 2008

Keywords:
Benzodiazepine receptor
[11C]flumazenil
[18F]flumazenil
Kinetic modeling
Positron emission tomography

ABSTRACT

[11C]Flumazenil is the reference radioligand for Positron Emission Tomography (PET) studies of central benzodiazepine (BZ) receptors. Fluorine is available in the flumazenil molecule and [18F]flumazenil has recently been prepared. The aim of the present PET-study in 8 male subjects was to examine the binding of [18F]flumazenil in the human brain by direct comparison with [11C]flumazenil. Each subject participated in two 93-minute PET-measurements with [11C]flumazenil and [18F]flumazenil, respectively. Data were analyzed using compartment models with metabolite-corrected arterial plasma input and reference tissue models using the pons as reference region. There was no evident difference between the kinetic behaviors of the two ligands. Overall, the noise in the time activity curves for [18F]flumazenil was lower at late time points, and the variance of the kinetic parameters was lower than for [11C]flumazenil. In BZ receptor rich regions, such as the neocortex, the 3-compartment model was statistically favored, whereas the 2-compartment model was favored in the pons. Binding potential values obtained by the reference tissue models were in good agreement with those obtained by the kinetic analysis. There was no support for the presence of specific binding in the pons. In conclusion, the binding and the kinetic behavior of [11C]flumazenil and [18F]flumazenil were similar. The present analysis supports the use of pons as reference region in simplified protocols without arterial blood sampling. [18F]flumazenil should thus be an excellent choice for applied studies at centers not having a cyclotron.

Introduction

The γ-aminobutyric acid (GABA) neurotransmission system is of interest in the pathophysiology and pharmacological treatment of several brain disorders such as epilepsia, anxiety and sleep. [11C]Flumazenil was the first radioligand developed for imaging of the $GABA_A$ system by positron emission tomography (PET) (Maziere et al., 1984; Persson et al., 1985). Flumazenil acts as an antagonist at the benzodiazepine binding site of $GABA_A$ receptors containing α1, α2, α3 or α5 subunits (Hammers, 2004). These four subunits are prevalent in the neocortex and the cerebellum. The binding of [11C]flumazenil in the human brain has been quantified using reference tissue models (Savic et al., 1988; Abadie et al., 1992), saturation studies (Pappata et al., 1988; Persson et al., 1989) and compartment model analyses with a metabolite-corrected plasma input function (Blomqvist et al., 1990; Koeppe et al., 1991; Price et al., 1993; Delforge et al., 1995; Millet et al., 2002). In clinical studies, [11C]flumazenil has been used to detect epileptic foci (Savic et al., 1988), and to examine patients with disorders such as Alzheimer's disease (Meyer et al., 1995), chronic alcoholic-dependency (Litton et al., 1993; Lingford-Hughes et al., 2005a) or amyotrophic lateral sclerosis (Turner et al., 2005). New fields of interest are cortical damage after stroke or trauma (Yamauchi et al., 2005; Beuthien-Baumann, et al., 2005) and the use of [11C]flumazenil to support drug development (Lingford-Hughes et al., 2005b).

In some studies, an F-18 labeled radioligand may be advantageous to C-11 due to physical half-life allowing longer data acquisition. Another advantage is that F-18 labeled ligands can be delivered to centers not having a cyclotron. As an alternative to [11C]flumazenil, fluorinated analogues of flumazenil, such as 5-(2′[18F]fluoroethyl) flumazenil ([18F]FEFMZ) (Moerlein and Perlmutter, 1992; Gründer et al., 2001), and 2′-[18F]fluoroflumazenil ([18F]FFMZ) (Yoon et al., 2003) have been proposed.

* Corresponding author. Niigata University Graduate School of Medicine and Dental Sciences, Division of Functional Imaging, Department of Sensory and Integrative Medicine, Asahimachi-dori Niigata, 951-8510, Japan. Fax: +81 25 227 0788.
E-mail address: ikuomi@aurora.ocn.ne.jp (I. Odano).

1053-8119/$ – see front matter © 2008 Elsevier Inc. All rights reserved.
doi:10.1016/j.neuroimage.2008.12.005

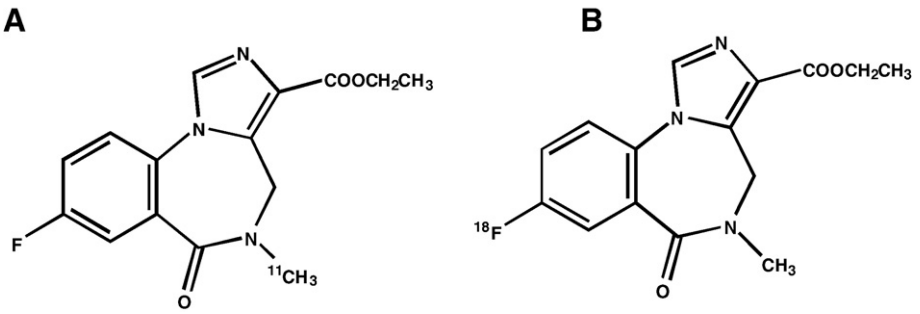

Fig. 1. Structures of [^{11}C]flumazenil (A) and [^{18}F]flumazenil (B).

Fluorine is however already available in the flumazenil molecule (Fig. 1). An advantage of radiolabeling in this position is that [^{18}F] flumazenil will be the same binding characteristics as [^{11}C]flumazenil. We have recently labeled flumazenil with fluorine for initial PET studies and demonstrated selective binding to benzodiazepine receptors in the monkey (Ryzhikov et al., 2005) and human brain (Odano et al., 2006 abstract).

The purpose of the present study was to examine the binding of [^{18}F]flumazenil in the human brain and to estimate binding parameters obtained by several invasive and non-invasive quantitative approaches. The binding of [^{18}F]flumazenil and [^{11}C]flumazenil was compared in eight control subjects, and some unresolved issues regarding reference region approaches for [^{11}C]flumazenil were addressed. Specific attention was given to the pons, a reference region which in previous studies has shown discrepant results with regard to the presence of specific binding. Attempts were made to arrive at a recommendation for optimal protocols in applied clinical studies.

Materials and methods

Subjects

Eight men, aged 23–29 years, participated in the study after signing written informed consent in accordance with the Helsinki Declaration. They were healthy according to medical history, physical examination, blood screening analysis, magnetic resonance imaging (MRI) of the brain and did not use any medication. There was no history of psychiatric disorder or drug abuse. The study was approved by the Research Ethics and Radiation Safety Committees of the Karolinska University Hospital.

Radiochemistry

[^{11}C]Flumazenil was synthesized by methylation of the desmethyled precursor with [^{11}C]methyltriflate following a procedure described earlier (Nagren and Halldin, 1998). [^{11}C]Flumazenil was obtained in decay corrected radiochemical yield of 65–75% (EOB, based on $^{11}CH_3OTf$) with a specific radioactivity of 5400–25,000 Ci/mmol at time of injection.

No-carrier-added (n.c.a.) [^{18}F]flumazenil was prepared by a method reported previously (Ryzhikov et al., 2005). Briefly, the radioligand was produced via standard nucleophilic radiofluorination of the corresponding nitro-analog Ro 15-2344 employing the K^{18}F/kryptofix complex in DMF at 160 °C for 30 min. The final product was isolated by reverse phase HPLC purification (acetonitrile/0.01 M phosphoric acid 20:80 (v/v)) with a total synthesis time of 90 min and a radiochemical yield of 10–12% (decay corrected, EOB). Usually 1.5–3.5 GBq of [^{18}F]flumazenil were produced in one batch using 10–30 min bombardment with 30–35 beam intensity on the ^{18}F target (PET trace cyclotron, GEMS). [^{18}F]flumazenil was obtained with a specific radioactivity of 4200–15,000 Ci/mmol. The radioactivity and mass injected were 383±44 MBq (mean±s.d., n=8) and 0.36±0.28 μg for [^{11}C]flumazenil. The corresponding values for [^{18}F] flumazenil were 199±45 MBq and 0.29±0.19 μg.

MRI and the head fixation system

T_1-weighted MR images were acquired using a 1.5 T Signa unit (General Electric, Milwaukee). A standard spin-echo sequence with a 256×256 matrix and 1 mm slice thickness was used with a repetition time of 400 ms. Echo times were 9 ms for images. A head fixation system was used both for MRI and PET measurements (Bergstrom et al., 1981). The MR images were transferred to a Unix workstation (Silicon Graphics, Inc., Mountain View, CA), and reconstructed into entire continuous images parallel to the AC–PC line using SPM2 and Matlab (Friston, 1994). The PET images were co-registered on the reconstructed MR images and resliced with a 2-mm thickness.

PET experimental procedure

The PET system used was Siemens ECAT Exact HR, which was run in 3D mode. The intrinsic resolution is 3.8 mm in plane and 4.0 mm axially at full width at half maximum (Wienhard et al., 1994). The reconstructed volume was displayed as 47 sections with a center-to-center distance of 3.125 mm. On three out of eight subjects, we performed [^{11}C]flumazenil studies in the morning and [^{18}F]flumazenil studies in the afternoon with an interval of about 3 h. On the other five subjects, [^{11}C]flumazenil studies were followed by a [^{18}F]flumazenil study on a separate day.

In each PET measurement, the subject was placed recumbent with his head in the PET system. A cannula was inserted into the left brachial artery and another into the right antecubital vein. A solution containing [^{11}C]flumazenil or [^{18}F]flumazenil (3 mL of mixture of ethanol/propylene glycol 30/70 and 5 mL physiological phosphate

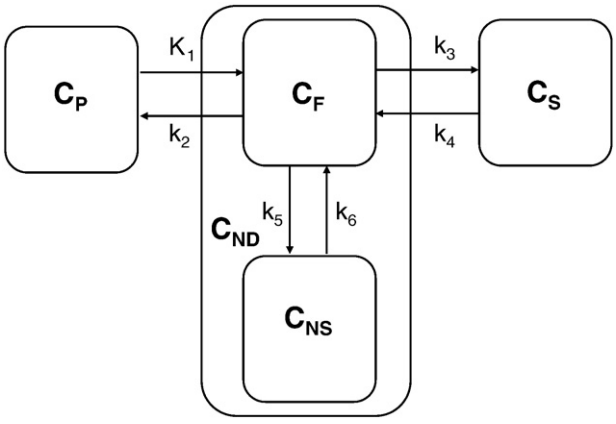

Fig. 2. The four-compartment model (4CM) used to describe the kinetics of [^{11}C] flumazenil and [^{18}F]flumazenil in the brain.

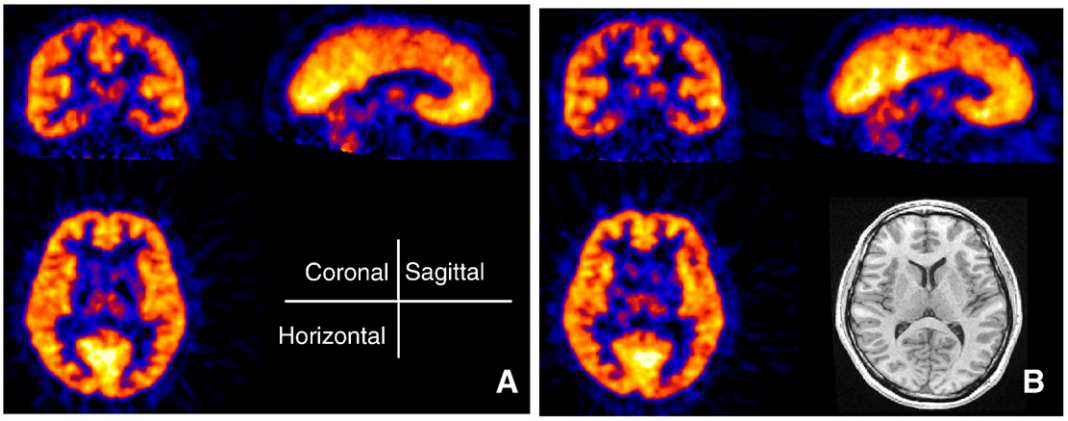

Fig. 3. Summation images of [^{11}C]flumazenil (A) and [^{18}F]flumazenil (B) of Subject A from 0 to 93 min after i.v. injection. Coronal, sagittal, horizontal and T_1-weighted MR images are shown. Note no uptake of both radioligands in the skull, which is evident by visual inspection of PET and MR images.

buffer, pH 7.4) was injected as a bolus during 2 s into the right antecubital vein. The cannula was then immediately flushed with 10 mL saline. After injection, brain radioactivity was measured in a series of consecutive time frames for 93 min. The frame sequence consisted of 12 fifteen-second frames, 3 one-minute frames, 3 three-minute frames and 13 six-minute frames.

Arterial blood sampling

To obtain the arterial input function, an automated blood sampling system (ABSS; Scanditronix, Uppsala, Sweden) was used during the first 5 min of each PET measurement. After the first 5 min, arterial blood samples (2 mL) were taken manually at the midpoint of each frame until the end of the measurement (Farde et al., 1989).

Plasma metabolite analysis (HPLC) of [^{11}C]flumazenil and [^{18}F]flumazenil

Arterial blood samples (2 mL each) were collected at 4, 6, 8, 10, 20, 30, 40 and 50 min after i.v. injection of [^{11}C]flumazenil. For [^{18}F] flumazenil additional samples were collected at 60, 75 and 90 min. The *in vivo* assay of radioactive metabolites was performed using standard procedures developed at Karolinska Institutet for new PET radioligands (Halldin et al., 1995). In short, plasma proteins were precipitated by addition of 0.7 mL of acetonitrile to 0.5 mL of the plasma sample. Blood was centrifuged (2000 ×*g* for 3 min) and the supernatant was analyzed by gradient HPLC under following conditions: C-18 μ-Bondapak column (Waters), 300×7.8 mm, 10 μ, mobile phase (gradient): ACN/0.01 M H_3PO_4; 0 min 15:85; 3 min 20:80; 7 min 60:40;10 min 15:85; flow rate 6 mL/min; UV 254 nm. HPLC analytical procedure was the same for both radioligands. Radioactivity of the injected supernatant and collected radioactivity from HPLC were measured with a NaI well counter for calculation of total recovery of the metabolite analysis.

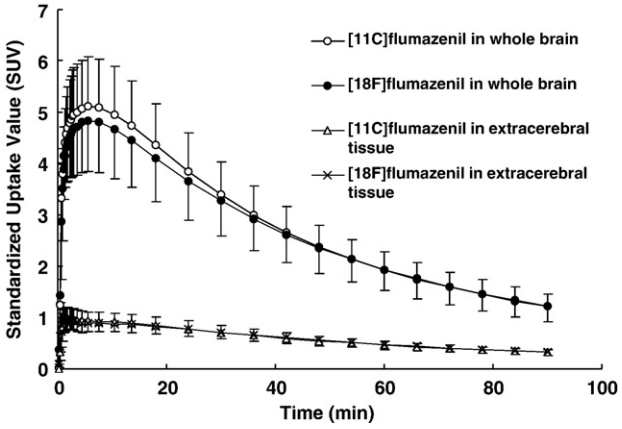

Fig. 4. The standardized uptake values (SUVs) (mean ± s.d., $n=8$) of [^{11}C]flumazenil and [^{18}F]flumazenil in whole brain and extracerebral tissue at the level of the basal ganglia are shown. The SUVs were calculated from the tissue radioactivity (Bq/mL) and the individual radioactivity injected (Bq).

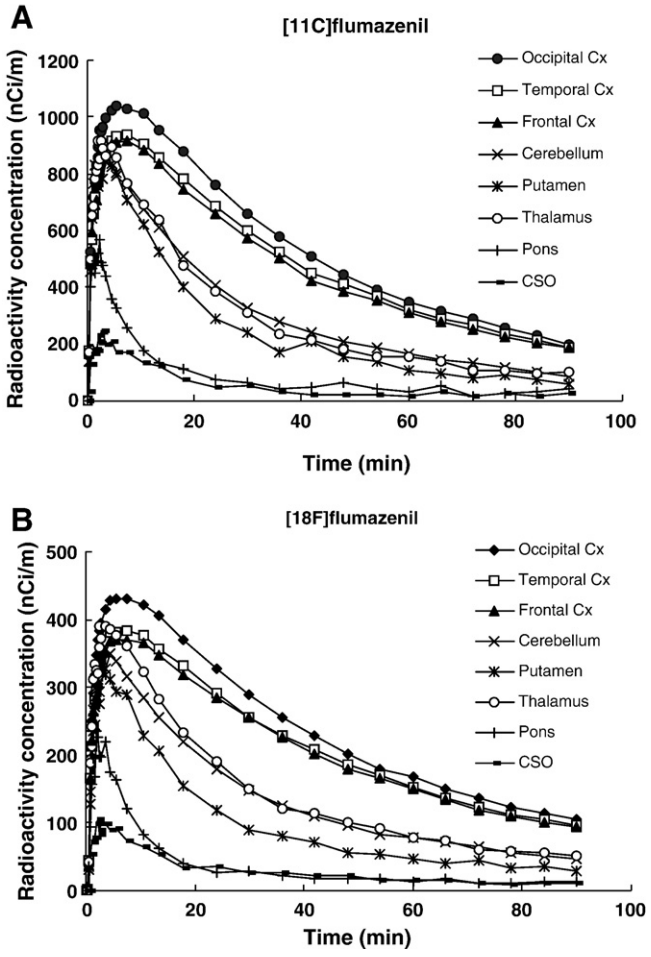

Fig. 5. Time-activity curves for regional bran radioactivity after intravenous injection of 400 MBq of [^{11}C]flumazenil (A) and 150 MBq of [^{18}F]flumazenil (B) in Subject A. The centrum semiovale (CSO) was a representative of white matter.

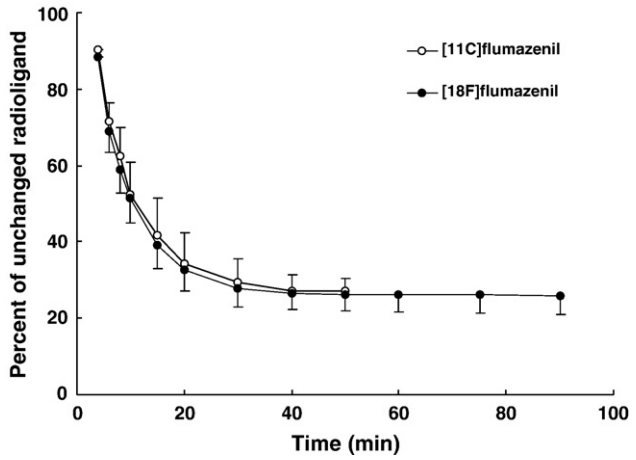

Fig. 6. Percent radioactivity in plasma representing unchanged radioligand after i.v. injection of [^{11}C]flumazenil and [^{18}F]flumazenil, respectively (mean ± s.d., n=8).

Regions of interest

Regions of interest (ROIs) were drawn manually on MR images by determination of frontal, temporal and occipital cortices, the putamen, the thalamus, the cerebellum and the pons. The centrum semiovale was chosen as a representative region for white matter. At the level of the basal ganglia, regions were also drawn for the whole brain, and for extracerebral tissue regions including the skull, vessels, muscles and subcutaneous tissue.

Standardized uptake value (SUV)

To assess the uptake of radioligands in the brain and to examine whether [^{18}F]flumazenil or [^{18}F]fluorine accumulates in the skull, standardized uptake values (SUVs) were obtained. The definition of SUV is radioactivity (Bq/mL)×body-weight (g)/injected dose (Bq) (Zasadny and Wahl, 1993; Sadato et al., 1998). The values were calculated by using the radioactivity of the whole brain and of extracerebral tissue as described above.

Invasive and non-invasive approaches

To examine [^{11}C]flumazenil and [^{18}F]flumazenil binding in brain, we employed several established quantitative approaches. Kinetic compartment analysis and linear graphical analysis are two approaches dependent on a metabolite-corrected arterial plasma curve as input function. The non-invasive linear graphical analysis and Simplified Reference Tissue Model (SRTM) using the pons as a reference region are referred to as reference tissue approaches.

Kinetic analysis with the three-compartment model (3CM)

[^{11}C]Flumazenil and [^{18}F]flumazenil was assumed to be freely diffusible from the blood pool to brain tissue. The kinetic behavior of the two radioligands was initially analyzed using the conventional four-compartment model as shown in Fig. 2 (Koeppe et al., 1991; Farde

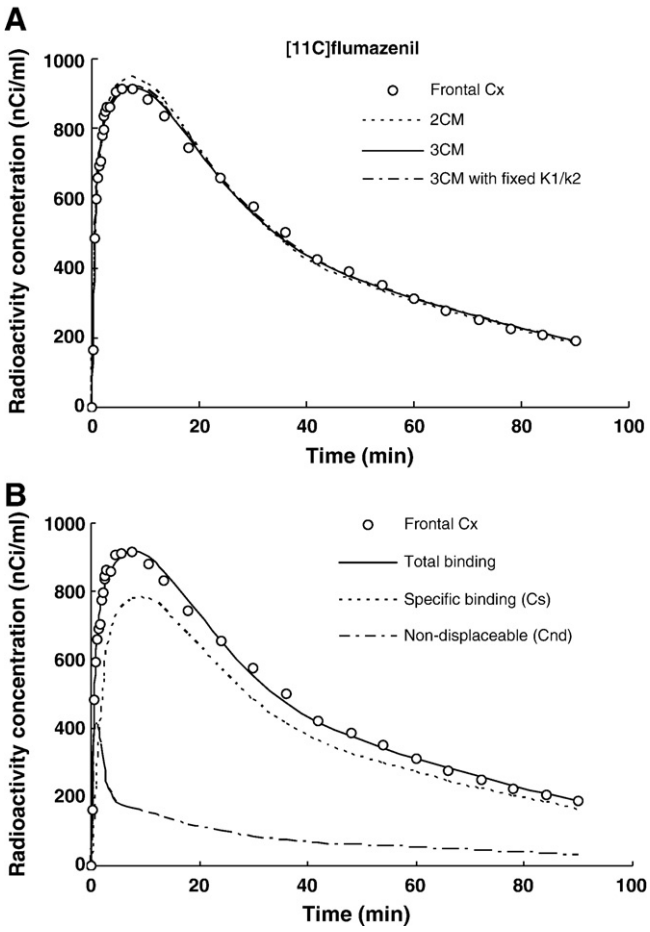

Fig. 7. (A) Radioactivity vs. time in the frontal cortex after i.v. injection of [^{11}C] flumazenil, and curve fits of the 2CM, the 3CM, and the 3CM with a fixed K_1/k_2 ratio obtained from pons (Subject A). (B) Total binding, specific binding and nondisplaceable ligand concentration in the frontal cortex as estimated by the 3CM.

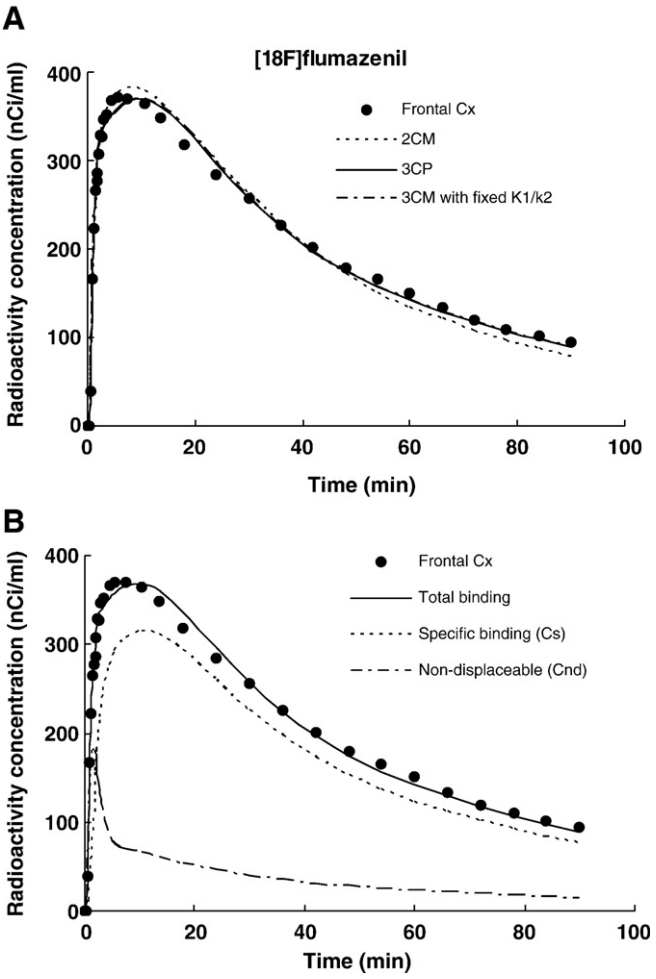

Fig. 8. (A) Radioactivity vs. time in the frontal cortex after i.v. injection of [^{18}F] flumazenil, and curve fits of the 2CM, the 3CM, and the 3CM with a fixed K_1/k_2 ratio obtained from pons (Subject A). (B) Total binding, specific binding and nondisplaceable ligand concentration of the frontal cortex as estimated by the 3CM.

et al., 1998). The four compartments correspond to the radioactivity concentrations of unchanged radioligand in plasma (C_P), free (unbound) radioligand in brain (C_F), nonspecifically bound radioligand (C_{NS}) and radioligand specifically bound to receptors (C_S). The rate constants K_1 and k_2 correspond to the influx and outflux rates of the radioligand across the blood–brain barrier, respectively. The rate constants k_3 and k_4 correspond to the rates for radioligand transfer between the compartments for free and specific radioligand binding to receptors, respectively. The rate constants for k_5 and k_6 correspond to the rates for radioligand transfer between the compartments for free and nonspecifically bound radioligand. All concentrations are expressed in units of nCi/mL. K_1 has units of mL/min/mL of brain tissue and k_2 through k_6 have units of min^{-1}.

To decrease variations of parameters, a common assumption was applied, in which the two compartments C_F and C_{NS} rapidly reach steady state to form one effective compartment (Wong et al., 1986; Logan et al., 1987; Lundberg et al., 2005). The resulting compartment (C_{ND}) corresponds to nondisplaceable radioligands in brain. The simplified model with three compartments and four first-order rate constants, K_1, k_2, k_3 and k_4 (Mintun et al., 1984; Huang et al., 1986), was used to describe the regional time radioactivity curves (TACs) for [^{11}C]flumazenil and [^{18}F]flumazenil binding.

On the basis of this model, the following first-order differential equations can be expressed:

$$\frac{dC_{ND}(t)}{dt} = K_1 \cdot C_P(t) - (k_2 + k_3) \cdot C_{ND}(t) + k_4 \cdot C_S(t), \quad (1)$$

$$\frac{dC_S(t)}{dt} = k_3 \cdot C_{ND}(t) - k_4 \cdot C_S(t), \quad (2)$$

and

$$C_T(t) = C_{ND}(t) + C_S(t), \quad (3)$$

where $C_T(t)$ is the total radioactivity concentration in brain obtained by the PET system. The time curves for radioactivity of unchanged [^{11}C]flumazenil and [^{18}F]flumazenil in arterial plasma, i.e., the metabolite-corrected arterial plasma curves, were used as input function, following correction for radioactivity in the cerebral blood volume. The net radioactivity concentration in brain, $C^{PET}_{tissue}(t)$, was thereby obtained according to the equation:

$$C^{PET}_{tissue}(t) = (1 - V_b) \cdot C_T(t) + V_b \cdot C_a(t), \quad (4)$$

where $C_a(t)$ is the radioactivity concentration in the whole blood, and V_b is the blood volume component, value which has been

Table 1
Comparison of rate constants obtained by fitting of the 2CM and 3CM to [^{11}C]flumazenil binding in the frontal cortex of eight subjects

Subject		$K1$		$k2$		$k3$		$k4$		$k1/k2$		$k3/k4$		DV_{total}	%COV	RSS	AIC	SC	F-statistics
		(mL/mL/min)	%COV	(min^{-1})	%COV	(min^{-1})	%COV	(min^{-1})	%COV		%COV	(BP)	%COV						2CP/3CP
A	2CM	0.353	3.4	0.067	3.3					5.3	1.9					25097	318	321	
	3CM	0.455	3.6	0.504	17.2	0.980	16.3	0.200	12.8	0.9	14.2	4.9	17.0	5.3	1.3	8779	289	295	$p<0.0001$
	3CM(2)	0.457	2.2	0.531		1.061	4.5	0.205	5.1	0.9		5.2	1.3	5.3	1.1	8952	290	296	$p<0.0001$
B	2CM	0.290	5.4	0.059	6.0					4.9	3.5					89640	358	360	
	3CM	0.433	4.8	0.723	6.8	0.867	16.2	0.116	7.4	0.6	10.3	7.5	11.3	5.1	1.4	9907	293	299	$p<0.0001$
	3CM(2)	0.432	3.6	0.722		0.871	6.0	0.117	6.4	0.6		7.5	1.4	5.1	1.2	9642	292	298	$p<0.0001$
C	2CM	0.400	2.3	0.084	3.6					4.8	2.8					42465	334	337	
	3CM	0.607	3.9	0.832	9.4	0.940	16.8	0.165	10.2	0.7	7.5	5.7	10.4	4.9	2.1	18336	312	318	$p<0.0001$
	3CM(2)	0.595	3.5	0.812		0.972	7.0	0.171	7.7	0.7		5.7	2.1	4.9	1.8	17583	311	317	$p<0.0001$
D	2CM	0.331	1.3	0.048	2.5					6.8	2.0					37282	330	333	
	3CM	0.419	5.5	0.436	37.4	0.999	51.6	0.161	15.4	1.0	40.1	6.2	44.4	6.9	2.4	19257	314	320	$p<0.0005$
	3CM(2)	0.424	3.1	0.458		1.004	11.7	0.155	12.2	0.9		6.5	1.9	6.9	1.6	28083	326	331	$p<0.05$
E	2CM	0.304	11.6	0.045	10.2					6.7	5.0					90181	358	361	
	3CM	0.336	17.5	0.362	74.2	1.796	14.2	0.281	54.6	0.9	57.0	6.4	68.6	6.8	2.8	15708	308	313	$p<0.0001$
	3CM(2)	0.345	2.0	0.371		1.460	2.2	0.229	3.1	0.9		6.4	2.0	6.9	1.7	15834	308	314	$p<0.0001$
F	2CM	0.309	4.1	0.053	5.0					5.8	4.0					156207	375	378	
	3CM	0.471	3.7	0.526	14.4	0.491	13.5	0.086	4.7	0.9	8.9	5.7	10.3	6.0	1.3	11670	298	304	$p<0.0001$
	3CM(2)	0.492	2.0	0.626		0.551	4.1	0.084	4.5	0.8		6.5	1.3	5.9	1.1	12504	300	306	$p<0.0001$
G	2CM	0.401	1.7	0.055	3.0											68428	349	352	
	3CM	0.555	5.1	0.556	31.8	0.878	30.3	0.138	8.3	1.0	27.3	6.4	31.7	7.4	1.2	17769	311	317	$p<0.0001$
	3CM(2)	0.559	2.0	0.559		0.853	5.6	0.134	6.0	1.0	1.0	6.4	1.3	7.4	1.2	19630	314	320	$p<0.0001$
H	2CM	0.435	2.0	0.077	3.1					5.6	2.5					67263	349	351	
	3CM	0.547	8.4	0.497	35.1	0.994	25.5	0.236	24.0	1.1	28.3	4.2	35.0	5.7	1.9	32130	330	335	$p<0.0001$
	3CM(2)	0.553	3.1	0.502		0.958	11.8	0.228	12.2	1.1		4.2	2.4	5.7	2.0	36032	333	339	$p<0.0005$
Mean	2CM	0.353	4.0	0.061	4.6					5.7	3.1								
	S.d.	0.054	3.4	0.014	2.6					0.8	1.1								
	3CM	0.478	6.6	0.555	28.3	0.993	23.1	0.173	17.2	0.9	24.2	5.9	28.6	6.0	1.8				
	S.d.	0.088	4.7	0.153	22.0	0.364	12.9	0.064	16.3	0.2	17.6	1.0	20.7	0.9	0.6				
	3CM(2)	0.482	2.7	0.573		0.966	6.6	0.165	7.1	0.9		6.0	1.7	6.0	1.5				
	S.d.	0.084	0.7	0.143		0.253	3.5	0.053	3.4	0.2		1.0	0.4	0.9	0.3				

2CM: two-compartment model.
3CM: three-compartment model.
3CM(2): three-compartment model with fixed $K1/k2$ for pons.
RSS: residual sum of squares.
AIC: Akaike information criterion.
SC: Schwarz criterion.

estimated to 0.04 (Farde et al., 1989; Koeppe et al., 1991; Delforge et al., 1995).

The four rate constants were determined by weighted non-linear least squares fitting technique with constraints restricting parameters between 0 to 1.0 for K_1 and k_2, 0 to 8.0 for k_3 and k_4 using the algorithm of Marquardt (1963) as implemented in the PMOD software version 2.85 (PMOD Technologies Ltd., Zurich, Switzerland). To decrease the dependency of the initial value chosen for the fitting procedure, the Simplex algorithm (Caceci and Cacheris, 1984) was applied to determine the initial values.

We also used the three-compartment model (3CM) to fit the TACs for the pons. The assumption is that the pons is a structure in brain having a negligible density of benzodiazepine receptors. The second tissue compartment was assumed to reflect nonspecific instead of specific binding. In this case, the parameters k_3 and k_4 were interpreted as k_5 and k_6, respectively.

Binding potential

After injection of a radioligand with high specific radioactivity, it is not possible to differentiate the receptor density (B_{max}) and affinity (K_D). The B_{max} to K_D ratio correspond to the ratio of k_3 and k_4 in the 3CM, and is referred to as the binding potential (Mintun et al., 1984). The binding potential (BP) is defined as follows:

$$BP = f_{ND} \cdot \frac{B_{max}}{K_D} = \frac{k_3}{k_4}, \quad (5)$$

where, f_{ND} is the free fraction of radioligand in the nondisplaceable compartment (Innis et al., 2007), the term of which is equal to f_2. Since the fraction of radioligand which is unbound to plasma proteins was not measured in the present studies, the value of f_{ND} was not included in the analysis.

Distribution volume

[^{11}C]Flumazenil and [^{18}F]flumazenil binding was also described using the concept of "total distribution volume", DV_{total}, which is defined by the following equation (Koeppe et al., 1991; Lammertsma et al., 1996):

$$DV_{total} = \frac{K_1}{k_2}\left(1 + \frac{k_3}{k_4}\right). \quad (6)$$

The three-compartment model with fixed K_1/k_2 for pons (3CM fixed K_1/k_2)

In this configuration, the partition coefficient, K_1/k_2, was assumed to be equal in all brain regions. The K_1/k_2 ratio was obtained from the

Table 2
Comparison of rate constants obtained by fitting of the 2CM and 3CM to [^{18}F]flumazenil binding in the frontal cortex of eight subjects

Subject		*K*1		*k*2		*k*3		*k*4		*k*1/*k*2		*k*3/*k*4		DV_{total}	%COV	RSS	AIC	SC	*F*-statistics
		(mL/mL/min)	%COV	(min^{-1})	%COV	(min^{-1})	%COV	(min^{-1})	%COV		%COV	(BP)	%COV						2CP/3CP
A	2CM	0.313	1.9	0.064	2.8					4.9	2.2					6894	278	281	
	3CM	0.420	3.2	0.496	9.9	0.786	9.6	0.162	9.5	0.8	8.0	4.9	9.9	5.0	1.3	2512	251	256	$p<0.0001$
	3CM(2)	0.454	3.2	0.536		0.632	7.7	0.129	8.4	0.8		4.9	2.2	5.0	1.8	3610	262	268	$p<0.0005$
B	2CM	0.351	2.8	0.065	3.6					5.4	3.0					17388	307	310	
	3CM	0.519	4.1	0.713	12.1	0.897	9.1	0.138	7.0	0.7	8.7	6.5	11.4	5.5	1.9	5643	276	282	$p<0.0001$
	3CM(2)	0.516	3.1	0.690		0.872	8.8	0.138	9.1	0.7		6.3	1.7	5.5	1.5	5578	275	281	$p<0.0001$
C	2CM	0.310	1.1	0.065	2.2					4.8	1.7					8786	286	288	
	3CM	0.386	4.5	0.551	20.4	1.352	18.5	0.227	15.9	0.7	18.0	6.0	20.9	4.9	1.6	4945	272	277	$p<0.0005$
	3CM(2)	0.386	3.0	0.498		1.351	15.6	0.227	15.3	0.8		6.0	2.1	5.4	1.8	4918	272	277	$p<0.0005$
D	2CM	0.315	2.2	0.059	3.3					5.4	2.9					20100	311	314	
	3CM	0.426	4.9	0.561	20.4	0.916	11.5	0.146	11.3	0.8	15.9	6.3	17.9	5.5	1.4	5998	278	283	$p<0.0001$
	3CM(2)	0.428	2.2	0.566		0.898	6.4	0.142	6.9	0.8		6.3	1.5	5.5	1.3	5503	275	281	$p<0.0001$
E	2CM	0.367	3.0	0.060	4.4					6.1	3.5					25087	318	321	
	3CM	0.543	3.1	0.560	15.1	0.598	10.6	0.108	9.2	1.0	3.1	5.6	4.1	6.4	2.3	10576	295	301	$p<0.0001$
	3CM(2)	0.525	4.2	0.495		0.556	21.3	0.111	20.2	1.1		5.0	3.0	6.4	2.5	9821	293	299	$p<0.0001$
F	2CM	0.348	1.4	0.067	2.3					5.2	1.7					8005	283	285	
	3CM	0.458	5.8	0.553	47.3	1.313	31.7	0.243	28.1	0.8	42.6	5.4	49.4	5.3	1.7	5476	275	281	$p<0.01$
	3CM(2)	0.416	2.9	0.489		1.392	13.0	0.270	12.7	0.9		5.2	1.4	5.2	1.4	5546	275	281	$p<0.01$
G	2CM	0.326	1.7	0.052	2.7					6.2	2.1					24638	317	320	
	3CM	0.449	2.4	0.507	11.1	0.790	8.2	0.128	5.6	0.9	8.9	6.2	10.6	6.3	0.8	11577	298	304	$p<0.0001$
	3CM(2)	0.444	1.2	0.501		0.817	2.7	0.133	3.0	0.9		6.2	0.9	6.3	0.7	2251	247	253	$p<0.0001$
H	2CM	0.309	1.6	0.057	3.1					5.4	2.3					9962	289	292	
	3CM	0.397	5.3	0.367	38.3	0.692	42.4	0.169	11.9	1.1	33.6	4.1	41.7	5.5	1.6	4145	266	272	$p<0.0001$
	3CM(2)	0.408	2.3	0.458		0.854	8.4	0.166	9.2	0.9		5.1	1.9	5.5	1.6	4777	271	276	$p<0.0001$
Mean	2CM	0.330	2.0	0.061	3.0					5.4	2.4								
	S.d.	0.022	0.7	0.005	0.7					0.5	0.7								
	3CM	0.450	4.2	0.539	21.8	0.918	17.7	0.165	12.3	0.8	17.3	5.6	20.8	5.5	1.6				
	S.d.	0.056	1.2	0.096	13.8	0.276	12.7	0.048	7.1	0.1	13.8	0.8	16.3	0.6	0.4				
	3CM(2)	0.447	2.8	0.529		0.921	10.5	0.165	10.6	0.9		5.6	1.8	5.6	1.6				
	S.d.	0.050	0.9	0.072		0.303	5.9	0.055	5.3	0.1		0.6	0.6	0.5	0.5				

2CM: two-compartment model.
3CM: three-compartment model.
3CM(2): three-compartment model with fixed *K*1/*k*2 for pons.
RSS: residual sum of squares.
AIC: Akaike information criterion.
SC: Schwarz criterion.

two-compartment model analysis of the pons, and was then entered into the 3CM analysis of each ROI.

Kinetic analysis with the two-compartment model (2CM)

If binding and dissociation at the specific binding compartment (C_S) are rapid compared to the transport parameters K_1 and k_2, the model can be reduced to two compartments. Thus, the single tissue compartment contain free, nonspecifically bound, and specifically bound ligand (Koeppe et al., 1991). In this manner, there will be only two rate constants, K_1 and k_2'. The rate constant k_2' corresponds to the efflux rate, and its relation to k_2, k_3 and k_4 of the 3CM is given by the following equation:

$$k_2' = \frac{k_2}{1 + k_3/k_4}. \quad (7)$$

Linear graphical approach (invasive)

[^{11}C]Flumazenil and [^{18}F]flumazenil binding was also analyzed using a invasive linear graphical analysis for reversible ligand binding to receptors (Logan et al., 1990). The integrated metabolite-corrected arterial input function, normalized to $C_{ROI}(t)$, was plotted versus integrated total regional radioactivity in the tissue normalized to $C_{ROI}(t)$. The regional total distribution volume (DV_{region}) was determined from the slope of the linear plots. When distribution volume in the pons is used as reference, the binding potential, $BP_{invasive}$, was given by the following equation:

$$BP_{invasive} = \frac{DV_{ROI}}{DV_{pons}} - 1. \quad (8)$$

Linear graphical approach (non-invasive)

In the non-invasive linear graphic analysis, the pons was used as reference region. Radioactivity in this tissue region was integrated over time and normalized to the last frame for the tissue radioactivity. The integrated value was plotted vs. integrated and normalized radioactivity for the pons. For a reversible radioligand, this plot becomes linear and the asymptote of the slope equals to the distribution volume ratio DVR (Logan et al., 1996). The binding potential, $BP_{non\text{-}invasive}$ was estimated as:

$$BP_{non-invasive} = DVR - 1. \quad (9)$$

Simplified Reference Tissue Model (SRTM)

According to SRTM (Lammertsma and Hume, 1996; Gunn et al., 1998), the binding potential, BP_{SRTM}, is obtained by using the following equation:

$$C_t(t) = R_1 \cdot C_{ref}(t) + k_2\left(1 - \frac{R_1}{1 + BP_{SRTM}}\right) \cdot C_{ref}(t) \otimes \exp\left(-\frac{k_2 \cdot t}{1 + BP_{SRTM}}\right), \quad (10)$$

where, R_1 is the ratio of K_1/K'_1 (K_1: influx rate constant for the target tissue, K'_1: influx rate constant for the reference tissue), and $C_t(t)$ and $C_{ref}(t)$ are TACs for the target and reference tissue, respectively. In this approach, the pons was used as the reference tissue. The symbol ⊗ denotes the convolution integral. To obtain BP values and distribution volume using linear graphical analysis and simplified reference tissue models, we also used the PMOD software version 2.85. Blood volume correction was not performed in this approach, because it is not included in the soft ware.

Dispersion of the radioactivity of [^{11}C]flumazenil and [^{18}F]flumazenil

To examine the dispersion of radioactivity of [^{11}C]flumazenil and [^{18}F]flumazenil, the percent coefficient of variation (%COV) values of all ROIs described above were obtained. The values were calculated from mean and s.d. of radioactivity (nCi/mL) in the ROI placed on the axial PET images.

Sufficient time of data acquisition

To determine if shorter time of data acquisition might be sufficient in applied studies, mean % error and %COVs of BP values of the neocortex as a representative region were obtained by the 3CM with fixed K_1/k_2 for pons, non-invasive linear graphical analysis and SRTM. In this analysis, the BP value obtained by using the data for 93 min was regarded as the true value.

Statistics

Compartment model levels of complexity were compared using three statistical methods; the Akaike information criterion (Akaike, 1974), the Schwarz criterion (Schwarz, 1978) and *F*-statistics (Landaw and DiStefano 1984; Carson 1986; Farde et al., 1989). Statistical significance using the *F*-test was assumed for *P* values superior or equal to 0.05. The standard error of the parameter was given by the diagonal of the covariance matrix (Carson, 1986), expressed as percentage of the parameter value (coefficient of variation, %COV), and used to assess to validate the parameter by a non-linear least squares fitting procedure (Ginovart et al., 2006). Moreover, the BP and DV values for [^{11}C]flumazenil and [^{18}F]flumazenil obtained by each approach were compared using the paired *t*-test.

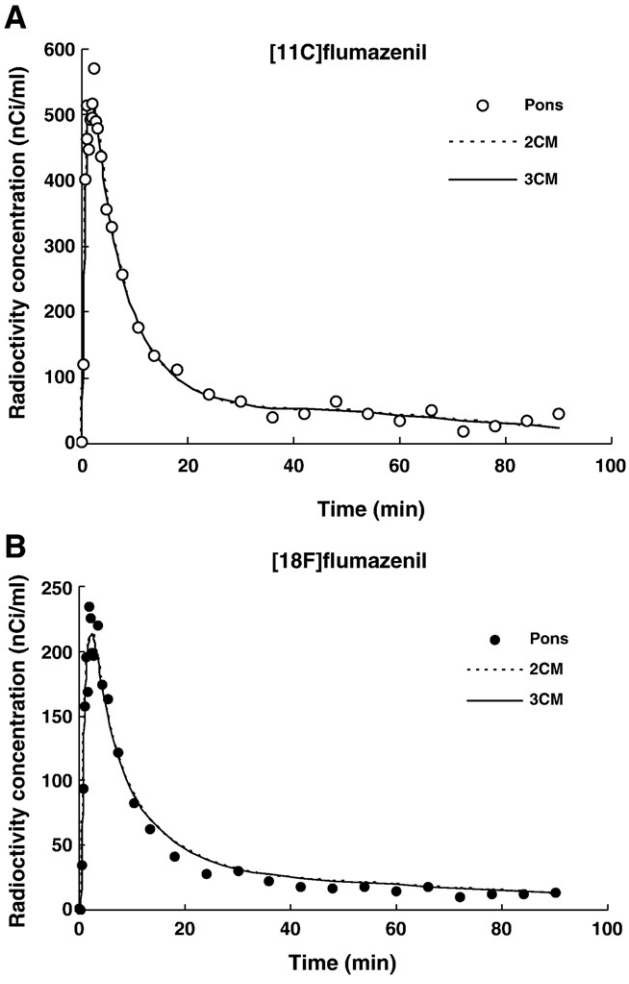

Fig. 9. Radioactivity vs. time in the pons after i.v. injection of [^{11}C]flumazenil (A) and [^{18}F]flumazenil (B), and curve fits of the 2CM and 3CM (Subject A).

Table 3
Comparison of rate constants obtained by fitting of the 2CM and 3CM to [^{11}C]flumazenil binding in the pons of eight subjects

Subject		*K*1		*k*2		*k*5		*k*6		*k*1/*k*2		*k*5/*k*6		DV_{total}	%COV	RSS	AIC	SC	*F*-statistics
		(mL/mL/min)	%COV	(min^{-1})	%COV	(min^{-1})	%COV	(min^{-1})	%COV		%COV	(BP)	%COV						2CP/3CP
A	2CM	0.329	3.2	0.382	5.2					0.9	2.9					15832	304	307	
	3CM	0.352	6.2	0.546	26.9	0.417	64.5	1.189	40.5	0.6	21.2	0.4	87.8	0.9	3.4	14918	306	312	ns
B	2CM	0.241	8.3	0.402	10.2					0.6	3.6					18591	309	312	
	3CM	0.263	13.0	0.613	84.4	0.441	369.0	1.042	148.5	0.4	73.0	0.4	237.0	0.6	5.8	17700	311	317	ns
C	2CM	0.338	2.6	0.462	3.8					0.7	2.9					12149	296	298	
	3CM	0.353	5.1	0.573	13.8	0.343	201.4	1.868	167.2	0.6	9.9	0.2	55.7	0.7	3.6	10622	295	301	ns
D	2CM	0.294	2.5	0.317	5.0					0.9	4.7					22660	315	318	
	3CM	0.308	17.5	0.438	153.4	0.901	531.1	2.765	200.0	0.7	137.4	0.3	562.3	0.9	4.1	21506	317	323	ns
E	2CM	0.192	2.9	0.205	5.8					0.9	5.9					33249	327	330	
	3CM	0.202	38.9	0.309	74.6	0.610	190.1	1.422	44.6	0.7	36.5	0.4	146.2	0.9	10.5	33785	331	337	ns
F	2CM	0.375	4.5	0.473	6.8					0.8	3.3					36988	330	333	
	3CM	0.384	8.5	0.629	12.9	0.720	29.1	2.176	35.3	0.6	16.1	0.3	55.8	0.8	4.2	36474	334	339	ns
G	2CM	0.422	2.9	0.419	2.0					1.0	2.6					15441	303	306	
	3CM	0.426	3.2	0.607	11.5	0.961	5.6	1.630	28.8	0.7	8.9	0.6	27.7	1.1	4.2	14606	305	311	ns
H	2CM	0.435	3.7	0.393	7.3					1.1						23347	316	319	
	3CM	0.440	7.2	0.452	103.3	0.785	839.8	5.928	81.4	1.0	97.2	0.1	829.7	1.1	3.8	25736	323	329	ns
Mean	2CM	0.328	3.8	0.382	5.5					0.9	3.7								
	S.d.	0.085	1.9	0.086	2.5					0.2	1.2								
	3CM	0.341	12.4	0.521	60.1	0.647	278.8	2.253	93.3	0.7	50.0	0.3	250.3	0.9	5.0				
	S.d.	0.081	11.6	0.112	52.4	0.232	288.7	1.586	68.3	0.2	47.6	0.1	291.7	0.2	2.3				

2CM: two-compartment model.
3CM: three-compartment model.
RSS: residual sum of squares.
AIC: Akaike information criterion.
SC: Schwarz criterion.
ns: no statistical significance.

Table 4
Comparison of rate constants obtained by fitting of the 2CM and 3CM to [^{18}F]flumazenil binding in the pons of eight subjects

Subject		*K*1		*k*2		*k*5		*k*6		*k*1/*k*2		*k*5/*k*6		DV_{total}	%COV	RSS	AIC	SC	*F*-statistics
		(mL/mL/min)	%COV	(min^{-1})	%COV	(min^{-1})	%COV	(min^{-1})	%COV		%COV	(BP)	%COV						2CP/3CP
A	2CM	0.277	3.1	0.327	5.0					0.8	4.3					4197	263	265	
	3CM	0.286	28.6	0.413	127.5	0.356	427.9	1.551	122.4	0.7	99.2	0.2	542.0	0.9	4.7	4283	267	273	ns
B	2CM	0.318	3.4	0.416	5.6					0.8	4.3					8201	283	286	
	3CM	0.322	24.0	0.511	198.2	0.447	1209.8	1.860	363.4	0.6	175.0	0.2	905.3	0.8	5.2	7578	285	291	ns
C	2CM	0.270	8.0	0.385	13.4					0.7	7.6					27353	321	324	
	3CM	0.275	21.0	0.502	38.3	0.695	350.6	2.507	125.2	0.5	54.2	0.3	227.6	0.7	12.2	28025	325	331	ns
D	2CM	0.332	3.5	0.440	6.5					0.8	4.3					11814	295	298	
	3CM	0.383	6.7	0.864	70.5	0.970	160.7	1.366	36.0	0.4	67.2	0.7	159.4	0.8	5.0	10742	296	301	ns
E	2CM	0.361	1.9	0.342	3.2					1.1	2.6					3841	260	263	
	3CM	0.365	12.0	0.437	94.2	0.900	416.1	3.169	152.1	0.8	87.1	0.3	395.7	1.1	3.7	3751	263	269	ns
F	2CM	0.321	3.5	0.378	5.9					0.8	3.5					6191	275	278	
	3CM	0.310	8.0	0.456	59.1	0.783	422.0	3.386	253.4	0.7	54.0	0.2	309.1	0.8	5.9	8534	289	294	ns
G	2CM	0.325	3.1	0.368	4.3					0.9	2.6					12134	296	298	
	3CM	0.363	17.9	0.746	104.5	0.999	187.6	1.122	14.6	0.5	87.1	0.9	191.0	0.9	4.8	11966	299	305	ns
H	2CM	0.290	3.0	0.329	5.6					0.9						3773	259	262	
	3CM	0.293	10.8	0.400	76.6	0.642	411.5	2.940	62.6	0.7	68.6	0.2	385.8	0.9	3.6	3733	263	269	ns
Mean	2CM	0.312	3.8	0.373	6.3					0.8	4.2								
	S.d.	0.031	1.8	0.041	3.1					0.1	1.7								
	3CM	0.325	16.1	0.541	96.1	0.724	448.3	2.238	141.2	0.6	86.5	0.4	389.5	0.9	5.6				
	S.d.	0.041	8.0	0.170	49.6	0.236	325.9	0.876	117.1	0.1	39.3	0.3	243.3	0.1	2.8				

2CM: two-compartment model.
3CM: three-compartment model.
RSS: residual sum of squares.
AIC: Akaike information criterion.
SC: Schwarz criterion.
ns: no statistical significance.

Results

Image comparisons of [^{11}C]flumazenil and [^{18}F]flumazenil

All eight subjects participated in the study according to the protocol. A representative summation image of brain radioactivity after [^{11}C]flumazenil and [^{18}F]flumazenil injected is shown in Fig. 3. The images are almost identical as expected. With time the sequential images of [^{11}C]flumazenil became more noisy than those of [^{18}F]flumazenil.

Cerebral and extracerebral uptake

The SUV curves of [^{11}C]flumazenil and [^{18}F]flumazenil are shown in Fig. 4. After i.v. injection of both radioligands, the brain uptake of radioactivity was rapid. The SUV curves for [^{11}C]flumazenil and [^{18}F]flumazenil were similar, and the peak SUV of whole brain was 4.9±0.9 (mean±s.d.) at 5.5 min for [^{11}C]flumazenil, and 4.6±0.9 for [^{18}F]flumazenil, respectively. The curves for extracerebral regions were also similar for [^{11}C]flumazenil and [^{18}F]flumazenil, and both mean SUVs were less than 1.0, showing that there was no bone uptake indicating accumulation of [^{11}C]fluorine or [^{18}F]fluorine, which is evident by visual inspection of PET and MR images in Fig. 3.

Time-activity curves for regional brain radioactivity

The regional TACs are shown in Fig. 5. Highest uptake was observed in the neocortical regions, intermediate uptake in the cerebellum, thalamus and putamen, and low uptake in the pons and centrum semiovale (CSO). There was no evident difference between TACs for the two radioligands.

Metabolite analysis

Both radioligands were rather rapidly metabolized. The fractions of unchanged radioligand in plasma are shown in Fig. 6. Low radioactivity in the plasma samples of [^{11}C]flumazenil after 50 min hampered analysis of radioactive metabolites in plasma at later time points. HPLC recovery for the analysis of radioactive metabolites of [^{11}C]flumazenil and [^{18}F]flumazenil was 92±3% and 97±3%, respectively, confirming that radioactivity injected eluted during the 10 min run time.

Kinetic analysis

The TACs for regional [^{11}C]flumazenil and [^{18}F]flumazenil binding could be described by the compartment analyses (Figs. 7 and 8). The rate constants and statistical comparisons of the curve fits are given in Tables 1 and 2 for the frontal cortex. The 3CM using fixed K_1/k_2 ratio derived from the pons provided robust estimates of the BP with low % COVs. There was no evident difference between binding parameters obtained with [^{11}C]flumazenil and [^{18}F]flumazenil. These observations were similar to those other neocortical regions as well as putamen, thalamus and cerebellum.

For the pons, the uptake curves of [^{11}C]flumazenil and [^{18}F]flumazenil were not statistically better described by the 3CM than by the 2CM. The fitted curves are shown in Fig. 9, and the rate constants and statistical comparison is given in Tables 3 and 4. In the statistical analysis, the Akaike information criterion and Schwarz

Table 5
Comparison of regional binding potential values and distribution volume estimates obtained with [^{11}C]flumazenil and [^{18}F]flumazenil in the brain (mean±s.d., n=8)

[^{11}C]flumazenil	Invasive approaches						Non-invasive approaches	
	Kinetic analysis				Linear graphical analysis		Logan DVR	SRTM
Region	$k3/k4$ %COV	DV %COV	$k3/k4$ (fixed $K1/k2$) %COV	DV %COV	BP_{Logan}	DV %COV	$BP_{non\text{-}invasive\ Logan}$	BP_{SRTM} %COV
Frontal	5.9±1.0	6.0±0.9	6.0±1.0	6.0±0.9	5.8±0.9	5.9±0.9	5.6±0.8	5.6±0.8
	29±21	1.8±0.6	1.7±0.4	1.5±0.3		0.2±0.1		2.3±0.6
Temporal	5.8±1.0	6.3±1.1	6.4±1.0	6.3±1.1	6.1±1.0	6.2±1.0	5.9±0.9	6.0±0.9
	33±25	1.7±0.5	1.7±0.5	1.4±0.4		0.6±0.6		2.5±0.6
Occipital	6.1±1.2	6.4±1.0	6.5±1.2	6.4±1.0	6.2±1.0	6.3±1.0	6.0±1.0	6.0±0.9
	32±49	1.7±0.5	1.7±0.5	2.3±2.2		0.6±0.7		2.2±0.5
Putamen	2.6±0.4	3.1±0.5	2.6±0.5	3.1±0.5	2.7±0.6	3.2±0.5	2.6±0.5	2.5±0.5
	29±21	3.0±1.1	3.6±0.6	2.4±0.9		0.5±0.3		5.2±0.4
Thalamus	2.9±0.7	3.3±0.4	2.8±0.6	3.3±0.4	2.8±0.7	3.3±0.5	2.7±0.6	2.7±0.6
	23±13	2.5±0.4	3.5±0.8	2.6±0.6		0.4±0.3		5.2±1.5
Cerebellum	3.6±0.5	3.9±0.8	3.6±0.8	3.9±0.8	3.5±0.8	4.0±0.8	3.4±0.8	3.4±0.7
	24±9.7	2.0±0.3	2.6±0.5	2.0±0.4		0.4±0.3		3.6±0.7
Pons	0.3±0.1*	0.9±0.2	NA	NA	NA	0.9±0.2	NA	NA
	250±292	5.0±2.3				0.3±0.2		

[^{18}F]flumazenil	Invasive approaches						Non-invasive approaches	
	Kinetic analysis				Linear graphical analysis		Logan DVR	SRTM
Region	$k3/k4$ %COV	DV %COV	$k3/k4$ (fixed $K1/k2$) %COV	DV %COV	BP_{Logan}	DV %COV	$BP_{non\text{-}invasive\ Logan}$	BP_{SRTM} %COV
Frontal	5.6±0.8	5.5±0.6**	5.6±0.6	5.6±0.5	5.6±0.6	5.4±0.6**	5.6±0.6	5.6±0.6
	21±16	1.6±0.4	1.8±0.6	1.6±0.5		0.2±0.1		2.5±0.5
Temporal	6.1±0.6	5.8±0.7**	6.0±0.8	5.9±0.6	6.0±0.7	5.7±0.7**	6.0±0.7	5.9±0.7
	17.5±18	1.6±0.4	1.8±0.6	1.5±0.5		0.2±0.1		2.6±0.6
Occipital	5.9±0.7	5.9±0.6**	6.0±0.6	5.9±0.5**	5.5±1.9	5.7±0.5**	6.2±0.7	5.6±1.3
	32±28	1.6±0.6	1.7±0.6	1.5±0.5		1.1±2.1		2.9±1.2
Putamen	2.6±0.5	2.8±0.4**	2.4±0.5	2.9±0.4	2.5±0.6	2.9±0.4**	2.5±0.6	2.4±0.5
	41±33	2.5±0.8	3.3±1.2	2.5±0.6		0.3±0.2		5.7±1.6
Thalamus	2.8±0.6	3.1±0.3	2.7±0.5	3.1±0.2	2.7±0.7	3.0±0.4	2.7±0.7	2.7±0.6
	48±57	2.7±0.6	3.5±1.0	2.5±0.6		0.3±0.2		5.3±1.6
Cerebellum	3.3±0.8	3.6±0.6**	3.3±0.6	3.7±0.6	3.4±0.7	3.6±0.6**	3.4±0.7	3.4±0.6
	23±28	2.2±0.5	2.7±0.6	2.1±0.4		0.3±0.3		4.0±1.1
Pons	0.4±0.3*	0.9±0.1	NA	NA	NA	0.8±0.1	NA	NA
	390±243	5.6±2.8				0.3±0.2		

$k3/k4$=BP, binding potential. DV: total distribution volume, SRTM: simplified reference tissue model. *$k5/k6$ for pons.
NA: not analyzed. **The DV values for [^{18}F]flumazenil were lower than those for [^{11}C]flumazenil ($p<0.05$).

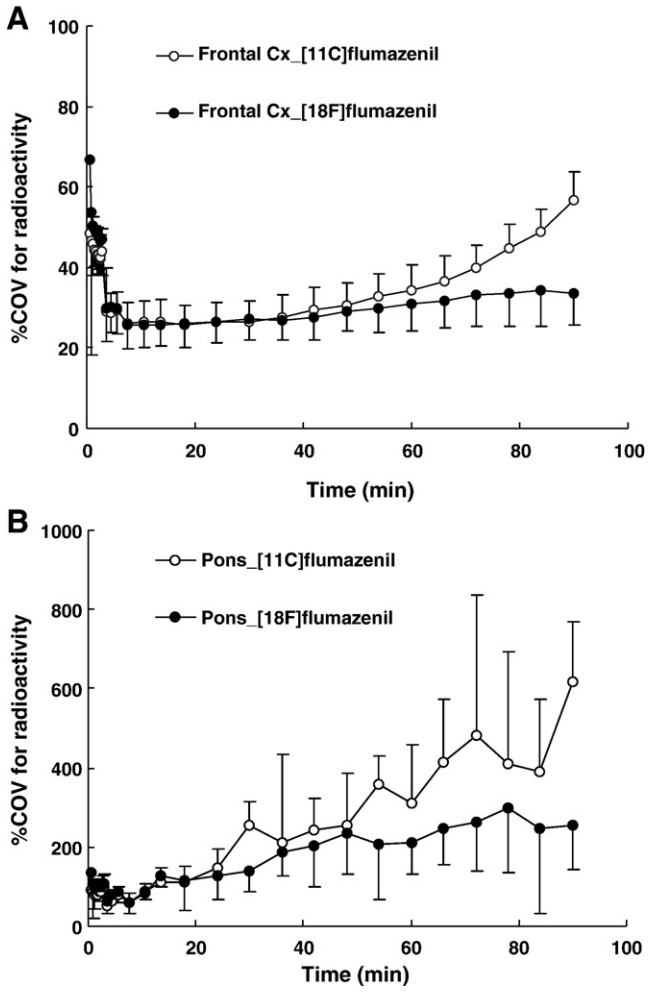

Fig. 10. Time curves showing percent COV for radioactivity in the frontal cortex (A) and pons (B) after i.v. injection of [^{11}C]flumazenil and [^{18}F]flumazenil (mean ± s.d., n=8).

criterion scores were lower for the two-compartment model than for the three-compartment model. Moreover, *F*-statistics rejected the null hypothesis, i.e. that the 3CM more adequately describes radioligand uptake.

Linear graphical analysis

In the graphical analysis, a linear phase was observed for all regions, including the pons. Theoretically, the slope of the fitted line corresponds to the total distribution volume, DV_{total}. The linear graphical analysis gave values for the binding potential in the range from 2.7 to 6.2 for [^{11}C]flumazenil, and 2.5 and 6.0 for [^{18}F]flumazenil as shown in Table 5. These values were not different from those obtained by the kinetic analysis.

Reference tissue models

The BP values obtained by the reference tissue models are for each region shown in Table 5. The values for [^{18}F]flumazenil were close to those for [^{11}C]flumazenil. Moreover, these values were similar to those obtained by the invasive approaches.

Statistical comparisons of the BP and DV values obtained with the two radioligands

When comparing the values for [^{11}C]flumazenil and [^{18}F]flumazenil binding parameters obtained by invasive and non-invasive approaches, there was no significant difference between the BP values for [^{11}C]flumazenil and [^{18}F]flumazenil (Table 5). The DV values for [^{18}F]flumazenil in the neocortical regions and putamen were however slightly lower than the DV-values for [^{11}C]flumazenil ($p<0.05$), when obtained by the kinetic analysis or the invasive linear graphical analysis. In the kinetic analysis with fixed K_1/k_2, there was no significant difference.

Dispersion of radioactivity

The time curves showing %COV of radioactivity in the frontal cortex and the pons were compared for [^{11}C]flumazenil and [^{18}F]flumazenil (Fig. 10). The values were obtained from mean and s.d. of the radioactivity measured by PET. The %COV values for [^{18}F]flumazenil were significantly lower than the values for [^{11}C]flumazenil calculated from approximately 50 min after radioligand injection ($p<0.05$), and onwards. These observations were similar to those for other regions.

Sufficient time of data acquisition

Three approaches, the 3CM with fixed K_1/k_2, non-invasive linear graphical analysis and SRTM, were examined with regard for time required to obtain stable estimates for the BP values (Table 6). The data

Table 6
Binding potential and percent errors (mean ± s.d.) for increasing time intervals after i.v. injection of dynamic data acquisition for [^{11}C]flumazenil and [^{18}F]flumazenil

[^{11}C]Flumazenil	3CM (fixed $K1/k2$)		Linear graphical analysis (non-invasive)		SRTM	
Time(min)	BP	% Error of BP	$BP_{non\text{-}invasive}$	% Error of BP	BP_{SRTM}	% Error of BP
10.5	5.3±0.9	16.0±2.9	4.6±2.0	27.4±34.0	5.9±1.3	12.6±6.8
18	5.5±1.1	13.5±3.9	6.5±1.3	10.0±8.7	5.7±1.0	6.3±3.3
30	5.8±1.0	7.6±3.5	6.4±1.1	8.1±5.3	5.8±1.0	4.2±2.3
48	6.1±1.0	3.0±1.4	6.1±0.8	3.9±2.9	5.9±0.9	1.6±1.2
60	6.2±1.0	1.5±0.7	6.0±0.8	3.7±2.8	5.9±0.9	1.5±1.0
72	6.3±1.1	0.6±0.4	6.0±0.8	2.5±2.1	5.9±0.8	0.8±0.6
90	6.3±1.1	0	5.9±0.9	0	5.9±0.9	0
[^{18}F]Flumazenil	3CM (fixed $K1/k2$)		Linear graphical analysis (non-invasive)		SRTM	
Time(min)	BP	% Error of BP	$BP_{non\text{-}invasive}$	% Error of BP	BP_{SRTM}	% Error of BP
10.5	4.7±0.6	20.8±6.0	5.7±1.2	20.3±19.9	7.2±1.8	39.2±22.2
18	5.2±0.5	12.8±4.3	6.4±1.2	10.7±8.6	5.8±0.4	7.6±4.1
30	5.5±0.6	6.6±2.6	6.1±1.0	6.4±4.6	5.6±0.7	5.4±3.4
48	5.8±0.6	3.5±2.7	6.0±0.8	2.4±2.5	5.8±0.7	2.1±1.2
60	5.8±0.6	2.5±3.3	6.0±0.8	1.9±2.6	5.8±0.7	1.1±0.5
72	5.9±0.6	2.0±2.9	6.0±0.7	1.0±1.0	5.8±0.7	0.5±0.4
90	5.9±0.6	0	5.9±0.6	0	5.8±0.6	0

The data for neocortex of eight subjects are shown. Note that the time interval 10.5–90 min was viewed as reference point in this comparative analysis.
BP: binding potential, SRTM: simplified reference tissue model.

for an average for frontal cortex are shown as a representative. The three approaches yielded similar BP values, which were stable from 30 min and onwards. The benefit from analyses based on longer data acquisition was a reduction in the % error of the BP.

Discussion

The binding of [^{11}C]flumazenil and [^{18}F]flumazenil in the human brain was examined and compared using several quantitative approaches. As has previously been reported for [^{11}C]flumazenil, the TACs could be well described by compartment analyses. The BP values obtained by the reference tissue models using pons as a reference region were in good agreement with those obtained by the kinetic analyses based on a metabolite-corrected plasma input function. The parameters obtained for the new radioligand [^{18}F]flumazenil were generally in good agreement with those for the reference radioligand [^{11}C]flumazenil. There is thus strong support for the view that [^{18}F]flumazenil is suitable for a majority of the applications established for [^{11}C]flumazenil. Due to the longer half-life of ^{18}F (110 min) an obvious exception is studies requiring repeated measurements on the same day.

It has been reported that binding parameters obtained by the 3CM with fixed K_1/k_2 for pons show favorably low variability (Price et al., 1993). The present analysis is in good agreement with this observation (Tables 1 and 2). It has moreover been proposed that radioactivity in the neocortex based on data after single injection of [^{11}C]flumazenil with high specific radioactivity can be adequately described by a 2CM (Koeppe et al., 1991; van Rij et al., 2005). However, by Scatchard analysis or multi-injection approaches using both high- and low-specific radioactivity of [^{11}C]flumazenil, TACs have been best described by a 3CM (Abadie et al., 1992; Price et al., 1993: Delforge et al., 1995; Millet et al., 2002). Our results support the latter view, since the TACs of [^{18}F]flumazenil and [^{11}C]flumazenil were statistically better described by the 3CM.

By contrast, the fits for the pons were not improved when the 3CM was used instead of the 2CM. A critical assumption for reference tissue models such as non-invasive graphical analysis and SRTM is that the radioligand kinetics of the reference tissue can be described by the 2CM (Maziere et al., 1984; Persson et al., 1985). When the assumption holds, the BP values will be almost identical to those obtained by the kinetic analysis using a metabolite-corrected plasma input function. It has, however, been suggested that some specific binding may occur in the pons (Delforge et al., 1995; Millet et al., 2002). The present observation that the pons was well described by the 2CM in all eight subjects (Tables 3 and 4) does not indicate specific binding this region. The reference tissue models using pons as reference region should thus be a suitable approach to obtain accurate binding potential values in routine clinical studies.

The BP values were robustly obtained by invasive and non-invasive approaches without significant difference between [^{11}C]flumazenil and [^{18}F]flumazenil (Table 5). However, the DV values for [^{18}F]flumazenil were lower ($p<0.05$) than those for [^{11}C]flumazenil. The DV concept is complex and dependent on the metabolite-corrected arterial input function. Since the difference was observed for almost all regions, a systematic error in the arterial input function for one of the radioligands cannot be excluded.

The variance for [^{18}F]flumazenil was lower than that for [^{11}C]flumazenil. Thus, the sequential images of [^{11}C]flumazenil became more noisy with time. As shown in Fig. 10, the %COV of radioactivity of [^{18}F]flumazenil is stable, but that of [^{11}C]flumazenil increases by time. The difference is most likely related to the physical aspect of the shorter half-life of Carbon-11 (20 min), when compared with Fluorine-18 (110 min).

Shorter time of data acquisition is an advantage in clinical applications. We examined the effect of time on the reliability of the BP values (Table 6). Assuming that lower than 5% of the mean percent error is acceptable, a time interval for dynamic data acquisition from 0 to 60 min could be sufficient to obtain reliable BP values not only for [^{11}C]flumazenil but also for [^{18}F]flumazenil.

Finally, there is another practical advantage for [^{18}F]flumazenil vs. [^{11}C]flumazenil. The longer half-life of [^{18}F] as compared with [^{11}C] could make the radioligand feasible to use at sites distant to radiopharmaceutical production. Once [^{18}F]flumazenil is synthesized, several PET examinations can be performed in 1 day using the same batch. These advantages might have a large impact in the availability of flumazenil-PET as a diagnostic modality for the evaluation of patients with drug-resistant epilepsy and other clinical investigations.

Conclusion

The binding parameters of [^{11}C]flumazenil and [^{18}F]flumazenil were similar thus supporting that [^{18}F]flumazenil can be used instead of [^{11}C]flumazenil in most studies. The reference tissue models using pons as reference region provided accurate values for the binding potential. Fluorine-18 labeled radioligands can be delivered to PET-centers not having a cyclotron. An advantage of [^{18}F]flumazenil is thus that the radioligand can be available for wider clinical use.

References

Abadie, P., Baron, J.C., Bisserbe, J.C., Boulenger, J.P., Rioux, P., Travere, J.M., Barre, L., Petit-Taboue, M.C., Zarifian, E., 1992. Central benzodiazepine receptors in human brain: estimation of regional B_{max} and K_D values with positron emission tomography. Eur. J. Pharmacol. 213, 107–115.

Akaike, H., 1974. A new look at the statistical model identification. IEEE Trans. Automat. Contr. AC-19, 716–723.

Bergstrom, M., Boethius, J., Eriksson, L., Greitz, T., Ribbe, T., Widen, L., 1981. Head fixation device for reproducible position alignment in transmission CT and positron emission tomography. J. Comput. Assist. Tomogr. 5, 136–141.

Beuthien-Baumann, B., Holthoff, V.A., Rudolf, J., 2005. Functional imaging of vegetative state applying single photon emission tomography and positron emission tomography. Neuropsychol. Rehabil. 15, 276–282.

Blomqvist, G., Pauli, S., Farde, L., Eriksson, L., Persson, A., Halldin, C., 1990. Maps of receptor binding parameters in the human brain—a kinetic analysis of PET measurements. Eur. J. Nucl. Med. 16, 257–265.

Caceci, M.S., Cacheris, W.P., 1984. Fitting curves to data, the Simplex algorithm is the answer. BYTE 9, 340–362.

Carson, R.E., 1986. Parameter estimation in positron emission tomography. In: Phelps, M.E., Mazziota, J.C., Schelbert, H.R. (Eds.), Positron Emission Tomography. Principles and Applications for the Brain and Heart. Raven Press, New York, pp. 347–390.

Delforge, J., Pappata, S., Millet, P., Samson, Y., Bendriem, B., Jobert, A., Crouzel, C., Syrota, A., 1995. Quantification of benzodiazepine receptors in human brain using PET, [^{11}C] flumazenil, and a single-experiment protocol. J. Cereb. Blood Flow Metab. 15, 284–300.

Farde, L., Eriksson, L., Blomquist, G., Halldin, C., 1989. Kinetic analysis of central [^{11}C] raclopride binding to D_2-dopamine receptors studied by PET—a comparison to the equilibrium analysis. J. Cereb. Blood Flow Metab. 9, 696–708.

Farde, L., Ito, H., Swahn, C.G., Pike, V.W., Halldin, C., 1998. Quantitative analyses of carbonyl-carbon-11-WAY-100635 binding to central 5-hydroxytryptamine-1A receptors in man. J. Nucl. Med. 39, 1965–1971.

Friston, K.J., 1994. Statistical parametric mapping. In: Thatcher, R.W., Hallett, M., Zeffiro, T., John, E.R., Huerta, M. (Eds.), Functional Neuroimaging. Academic Press, San Diego, pp. 79–93.

Ginovart, N., Meyer, J.H., Boovariwala, A., Hussey, D., Rabiner, E.A., Houle, S., Wilson, A.A., 2006. Positron emission tomography quantification of [^{11}C]-harmine binding to monoamine oxidase-A in the human brain. J. Cereb. Blood Flow Metab. 26, 330–344.

Gründer, G., Siessmeier, T., Lange-Asschenfeldt, C., Vernaleken, I., Buchholz, H.G., Stoeter, P., Drzezga, A., Lüddens, H., Rösch, F., Bartenstein, P., 2001. [^{18}F] Fluoroethylflumazenil: a novel tracer for PET imaging of human benzodiazepine receptors. Eur. J. Nucl. Med. 28, 1463–1470.

Gunn, R.N., Sargent, P.A., Bench, C.J., Rabiner, E.A., Osman, S., Pike, V.W., Hume, S.P., Grasby, P.M., Lammertsma, A.A., 1998. Tracer kinetic modeling of the 5-HT_{1A} receptor ligand [carbonyl-^{11}C]WAY-100635 for PET. NeuroImage 8, 426–440.

Halldin, C., Swan, C.-G., Farde, L., Sedvall, G., 1995. Radioligand disposition and metabolism — key information in early drug development. In: Comar, D. (Ed.), PET for Drug Development and Evaluation. Kluwer, Dordrecht, pp. 55–65.

Hammers, A., 2004. Flumazenil positron emission tomography and other ligands for functional imaging. Neuroimaging Clin. N. Am. 14, 537–551.

Huang, S.C., Barrio, J.R., Phelps, M.E., 1986. Neuroreceptor assay with positron emission tomography: equilibrium versus dynamic approaches. J. Cereb. Blood Flow Metab. 6, 515–521.

Innis, R.B., Cunningham, V.J., Delforge, J., Fujita, M., Gjedde, A., Gunn, R.N., Holden, J., Houle, S., Huang, S.C., Ichise, M., Iida, H., Ito, H., Kimura, Y., Koeppe, R.A., Knudsen, G.M., Knuuti, J., Lammertsma, A.A., Laruelle, M., Logan, J., Maguire, R.P.,

Mintun, M.A., Morris, E.D., Parsey, R., Price, J.C., Slifstein, M., Sossi, V., Suhara, T., Votaw, J.R., Wong, D.F., Carson, R.E., 2007. Consensus nomenclature for in vivo imaging of reversibly binding radioligands. J. Cereb. Blood Flow Metab. 27, 1533–1539.

Koeppe, R.A., Holthoff, V.A., Frey, K.A., Kilbourn, M.R., Kuhl, D.E., 1991. Compartmental analysis of [^{11}C]flumazenil kinetics for the estimation of ligand transport rate and receptor distribution using positron emission tomography. J. Cereb. Blood Flow Metab. 11, 735–744.

Lammertsma, A.A., Hume, S.P., 1996. Simplified reference tissue model for PET receptor studies. NeuroImage 4, 153–158.

Lammertsma, A.A., Bench, C.J., Hume, S.P., Osman, S., Gunn, K., Brooks, D.J., Frackowiak, R.S., 1996. Comparison of methods for analysis of clinical [^{11}C]raclopride studies. J. Cereb. Blood Flow Metab. 16, 42–52.

Landaw, E.M., DiStefano III, J.J., 1984. Multiexponential, multicompartmental, and noncompartmental modeling. II. Data analysis and statistical considerations. Am. J. Physiol. 246, R665–R677.

Lingford-Hughes, A., Wilson, S.J., Cunningham, V.J., Feeney, A., Stevenson, B., Brooks, D. J., Nutt, D.J., 2005a. GABA-benzodiazepine receptor function in alcohol dependence: a combined ^{11}C-flumazenil PET and pharmacodynamic study. Psychopharmacology 180, 595–606.

Lingford-Hughes, A., Wilson, S.J., Feeney, A., Grasby, P.G., Nutt, D.J., 2005b. A proof-of-concept study using [^{11}C]flumazenil PET to demonstrate that pagoclone is a partial agonist. Psychopharmacology 180, 789–791.

Litton, J.E., Neiman, J., Pauli, S., Farde, L., Hindmarsh, T., Halldin, C., Sedvall, G., 1993. PET analysis of [^{11}C]flumazenil binding to benzodiazepine receptors in chronic alcohol-dependent men and healthy controls. Psychiatry Res. 50, 1–13.

Logan, J., Wolf, A.P., Shiue, C.Y., Fowler, J.S., 1987. Kinetic modeling of receptor–ligand binding applied to positron emission tomographic studies with neuroleptic tracers. J. Neurochem. 48, 73–83.

Logan, J., Fowler, J.S., Volkow, N.D., Wolf, A.P., Dewey, S.L., Schlyer, D.J., MacGregor, R.R., Hitzemann, R., Bendriem, B., Gatley, S.J., 1990. Graphical analysis of reversible radioligand binding from time-activity measurements applied to [N-11C-methyl]-(-)-cocaine PET studies in human subjects. J. Cereb. Blood Flow Metab. 10, 740–747.

Logan, J., Fowler, J., Volkow, N.D., Wang, G., Ding, Y., Alexoff, D.L., 1996. Distribution volume ratio without blood sampling from graphical analysis of PET data. J. Cereb. Blood Flow Metab. 16, 834–840.

Lundberg, J., Odano, I., Olsson, H., Halldin, C., Farde, L., 2005. Quantification of ^{11}C-MADAM binding to the serotonin transporter in the human brain. J. Nucl. Med. 46, 1505–1515.

Marquardt, D.W., 1963. An algorithm for least-squares estimation of nonlinear parameters. Soc. Indust. Appl. Math. 11, 431–441.

Maziere, M., Hantraye, P., Prenant, C., Sastre, J., Comar, D., 1984. Synthesis of ethyl 8-fluoro-5,6-dihydro-5-[^{11}C]methyl-6-oxo-4H-imidazo[1,5-a][1, 4]benzodiazepine-3-carboxylate (Ro 15.1788-^{11}C): a specific radioligand for the *in vivo* study of central benzodiazepine receptors by positron emission tomography. Int. J. Appl. Radiat. Isot. 35, 973–976.

Meyer, M., Koeppe, R.A., Frey, K.A., Foster, N.L., Kuhl, D.E., 1995. Positron emission tomography measures of benzodiazepine binding in Alzheimer's disease. Arch. Neurol. 52, 314–317.

Millet, P., Graf, C., Buck, A., Walder, B., Ibánez, V., 2002. Evaluation of the reference tissue models for PET and SPECT benzodiazepine binding parameters. NeuroImage 17, 928–942.

Mintun, M.A., Raichle, M.E., Kilbourn, M.R., Wooten, G.F., Welch, M.J., 1984. A quantitative model for the in vivo assessment of drug binding sites with positron emission tomography. Ann. Neurol. 15, 217–227.

Moerlein, S.M., Perlmutter, J.S., 1992. Binding of 5-(2′-[^{18}F]fluoroethyl) flumazenil to central benzodiazepine receptors measured in living baboon by positron emission tomography. Eur. J. Pharmacol. 218, 109–115.

Nagren, K., Halldin, C., 1998. Methylation of amide and thiol functions with [^{11}C]methyl triflate, as exemplified by [^{11}C]NMSP, [^{11}C]flumazenil and [^{11}C]methionine. J. Label. Compd. Radiopharm. 41, 831–841.

Odano, I., Farde, L., Savic, I., Ciumas, C., Krasikova, R., Airaksinen, A., Gulyas, B., Pauri, S., Karlsson, P., Halldin, C., 2006. Central benzodiazepine receptor mapping with [^{18}F] flumazenil and PET-the first study in human brain. J. Nucl. Med. 47, 13p–14p.

Pappata, S., Samson, Y., Chavoix, C., Prenant, C., Maziere, M., Baron, J.C., 1988. Regional specific binding of [^{11}C]RO 15 1788 to central type benzodiazepine receptors in human brain: quantitative evaluation by PET. J. Cereb. Blood Flow Metab. 8, 304–313.

Persson, A., Ehrin, E., Eriksson, L., Farde, L., Hedstrom, C.C., Litton, J.E., Mindus, P., Sedvall, G., 1985. Imaging of [^{11}C]-labelled Ro 15-1788 binding to benzodiazepine receptors in the human brain by positron emission tomography. J. Psychiat. Res. 19, 609–622.

Persson, A., Pauli, S., Halldin, C., Stone-Elander, S., Farde, L., Sjogren, I., Sedvall, G., 1989. Saturation analysis of specific ^{11}C Ro 15-1788 binding to the human neocortex using positron emission tomography. Hum. Psychopharmacol. 4, 21–31.

Price, J.C., Mayberg, H.S., Dannals, R.F., Wilson, A.A., Ravert, H.T., Sadzot, B., Rattner, Z., Kimball, A., Feldman, M.A., Frost, J.J., 1993. Measurement of benzodiazepine receptor number and affinity in humans using tracer kinetic modeling, positron emission tomography, and [^{11}C]flumazenil. J. Cereb. Blood Flow Metab. 13, 656–667.

Ryzhikov, N.N., Seneca, N., Krasikova, R.N., Gomzina, N.A., Shchukin, E., Fedorova, O.S., Vassiliev, D.A., Gulyás, B., Hall, H., Savic, I., Halldin, C., 2005. Preparation of highly specific radioactivity [^{18}F]flumazenil and its evaluation in cynomolgus monkey by positron emission tomography. Nucl. Med. Biol. 32, 109–116.

Sadato, N., Tsuchida, T., Nakaumra, S., Waki, A., Uematsu, H., Takahashi, N., Hayashi, N., Yonekura, Y., Ishii, Y., 1998. Non-invasive estimation of the net influx constant using the standardized uptake value for quantification of FDG uptake of tumours. Eur. J. Nucl. Med. 25, 559–564.

Savic, I., Persson, A., Roland, P., Pauli, S., Sedvall, G., Widen, L., 1988. In-vivo demonstration of reduced benzodiazepine receptor binding in human epileptic foci. Lancet 2, 863–866.

Schwarz, G., 1978. Estimating the dimension of a model. Ann. Statist. 6, 461–464.

Turner, M.R., Osei-Lah, A.D., Hammers, A., Al-Chalabi, A., Shaw, C.E., Andersen, P.M., Brooks, D.J., Leigh, P.N., Mills, K.R., 2005. Abnormal cortical excitability in sporadic but not homozygous D90A SOD1 ALS. J. Neurol. Neurosurg Psychiatry 76, 1279–1285.

van Rij, C.M., Huitema, A.D., Swart, E.L., Greuter, H.N., Lammertsma, A.A., van Loenen, A. C., Franssen, E.J., 2005. Population plasma pharmacokinetics of ^{11}C-flumazenil at tracer concentrations. Br. J. Clin. Pharmacol. 60, 477–485.

Wienhard, K., Dahlbom, M., Eriksson, L., Michel, C., Bruckbauer, T., Pietrzyk, U., Heiss, W. D., 1994. The ECAT EXACT HR: performance of a new high resolution positron scanner. J. Comput. Assist. Tomogr. 18, 110–118.

Wong, D.F., Gjedde, A., Wagner Jr., H.N., 1986. Quantification of neuroreceptors in the living human brain. I. Irreversible binding of ligands. J. Cereb. Blood Flow Metab. 6, 137–146.

Yamauchi, H., Kudoh, T., Kishibe, Y., Iwasaki, J., Kagawa, S., 2005. Selective neuronal damage and borderzone infarction in carotid artery occlusive disease: a ^{11}C-flumazenil PET study. J. Nucl. Med. 46, 1973–1979.

Yoon, Y.H., Jeong, J.M., Kim, H.W., Hong, S.H., Lee, Y.S., Kil, H.S., Chi, D.Y., Lee, D.S., Chung, J.-K., Lee, M.C., 2003. Novel one-pot one-step synthesis of 2′-[(18)F]fluoroflumazenil (FFMZ) for benzodiazepine receptor imaging. Nucl. Med. Biol. 30, 521–527.

Zasadny, K.R., Wahl, R.L., 1993. Standardized uptake values of normal tissues at PET with 2-[fluorine-18]-fluoro-2-deoxy-D-glucose: variations with body weight and a method for correction. Radiology 189, 847–850.